Efficient I-V simulation of quantum devices using full bandstructure models.

R. Chris Bowen, Gerhard Klimeck, and William R. Frensley
Eric Jonsson School of Engineering and Computer Science
University of Texas at Dallas, Richardson, Texas 75083-0688

For several years it has been recognized that the single band effective mass model is insufficient to simulate quantum transport in material systems which are currently under investigation. This has prompted a growing effort on the part of theorists to include realistic bandstructures in quantum transport simulations. However, full bandstructure current-voltage calculations have proven to be numerically prohibitive. In this work we introduce an efficient technique to calculate current-voltage characteristics for quantum devices using tight-binding bandstructure models.

I. METHOD

Efforts to realize useful quantum devices have resulted in the investigation of a multitude of different material systems. The proliferation of new material systems has placed many demands on theorists trying to predict quantum transport behavior in these devices. In order to model quantum transport, it is necessary to include all of the relevant states which carriers may occupy. The quantum states in a crystal are described by its energy-momentum dispersion relationship or bandstructure. The majority of theoretical investigations of quantum devices to date have employed highly simplified models of bandstructure. However, it has become apparent that a more complete description of bandstructure must be incorporated into the transport models if we are to simulate many of the promising material systems which are currently under investigation. However, full bandstructure models require the inclusion of transverse basis states in the Hamiltonian making I-V simulations numerically prohibitive. The predominant obstacle in performing such calculations is the integration over extremely narrow spectral features arising from transmission resonances.

In this work we provide a solution to the problem of integration over transmission resonances. Our approach is to determine the position and width of the resonance lineshape by numerically locating the poles of the Green's function $G^R(E)$ in the complex energy plane. We have developed a shift and invert non-symmetric Lanczos algorithm which allows us to rapidly determine the location of these poles[1]. The complex energies associated with the poles provides the location and width of the sharp features in the transmission coefficient. With this information we obtain an energy grid which resolves these features and an analytic fit to the transmission characteristic. This information allows one to quickly calculate the current density in the device.

Using the location of these poles it is possible to generate accurate analytic fits for transmission lineshapes. We assume that the transmission coefficient may be approximated by a rational function.

$$t(E) = \frac{\prod_i (E - E^z{}_i)}{\prod_j (E - E^p{}_j)} = \prod_i (E - E^z{}_i) \left[\sum_j \frac{R_j}{(E - E^p{}_j)} \right] \quad (1)$$

Where E^p and E^z represent the location of the poles and zeros of $G^R(E)$ respectively. The partial fraction expansion coefficients (R_j) are treated as fitting parameters for the transmission lineshape. The real energy transmission amplitude is calculated at each pole location. These values are then used to calculate a unique set of partial fraction exapansion coefficients corresponding to the resonance lineshape. A comparison between our analytic fit and the exact transmission lineshape for a 34 Å GaAs/AlAs/GaAs barrier is shown in Figure 1. We have employed the $sp3s^*$ tight-binding bandstructure model in the numerical transmission calculation[2]. We have included a transmission zero (E^z=0) at zero energy in the analytic expansion in order to force the condition $t(0) = 0$. As illustrated in Figure 1, it is possible to obtain a rather accurate analytic fit to the transmission curve using only the locations of the poles and zeros of $G^R(E)$.

Our analytic fit is most accurate in the vicinity of the resonances where one would expect the trans-

0-7803-2442-0-8/95/$4.00

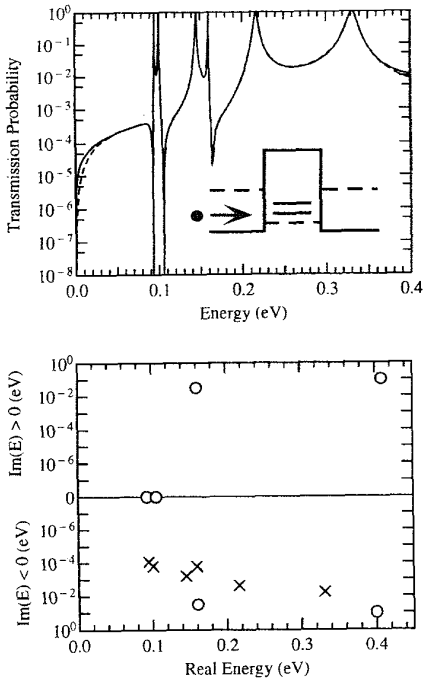

FIG. 1. (Top) Solid line: numerically calculated transmission coefficient vs. incident energy for a 34 Å GaAs/AlAs/GaAs barrier. The $sp3s^*$ tight-binding bandstructure model is employed in this simulation. Dashed line: analytic fit of the transmission coefficient using the partial fraction expansion shown in equation 1. Fano resonances are due to the coupling of the bound X-states with continuum Γ-states in the barrier. (Bottom) Poles (crosses) and zeros (circles) of $G^R(E)$ for this structure.

mission amplitude to be a rational function. In quantum devices the majority of current flow occurs at energies that are in the vicinity of the resonances. We may therefore obtain a good approximation for the current density by integrating our analytic fit. To calculate current densities we invoke the widely used single integral approximation using the analytic fit for t(E).

$$J(V) = \frac{e m^* k_B T}{2\pi^2 \hbar^3} \int_0^\infty dE \; |t(E,V)|^2 \; ln\left(\frac{1 + e^{(E_F - E)/k_B T}}{1 + e^{(E_F - E - eV)/k_B T}} \right) \quad (2)$$

We find the natural linewidths of some structures to be as sharp as 1neV and we would like to point out that adaptive integration schemes (which are typically used for this problem) tend to completely miss extremely sharp resonance features unless the required precision of the integration is set very high. These algorithms add energy nodes based on trial and error and measure the relative error of the addition of nodes into a certain integration region. This integration region is then divided into segments and these segments are again analyzed with the addition of nodes. This results in the addition of numerically expensive nodes in energy ranges where the absolute integral contribution is insignificant. However this numerical search for resonances is necessary, since the energetic location of these spectral features is unknown a'priori. Not only is the adaptive search for resonances expensive, it is also prohibitive for long structures containing multiple wells, like superlattices, since round-off errors in structures with many phaseshifts accumulate and create a noisy baseline, in which sharp resonances have to be found.

We generate an inhomogeneous energy grid which resolves the sharp resonances, the conduction band edges and the carrier distributions. Our energy grid is optimized for the minimization of the absolute error of the integral contributions and we therefore only place nodes where the integral contributions are significant. The inhomogeneous grid is structured such that the individual integral contributions are of the same order of magnitude, therefore minimizing numerical round-off errors. We find satisfactory answers for typically 50 energy nodes per resonance. We have also implemented adaptive grid generation schemes which can be used for the improvement of the originally fixed energy grid.

The resonance locator and analytic current density calculation have been incorporated into an in-

teractive multiband simulator which allows for rapid quantum device design.

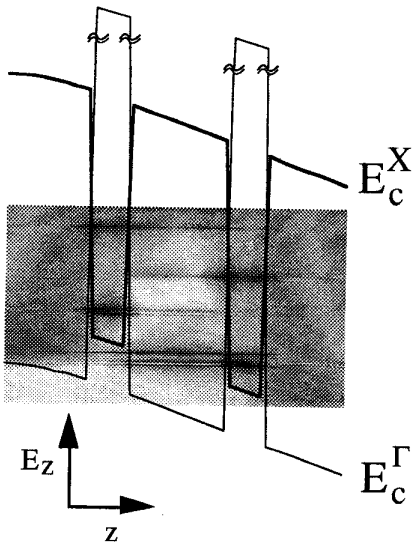

FIG. 2. Conduction band profile and density of states for GaAs/AlAs resonant tunneling diode. Additional resonant channels through X-states in the barrier are apparent in the density of states.

II. RESULTS

We shall first demonstrate our techniques on a GaAs/AlAs resonant tunneling diode (RTD) and compare these results to experimental data. The band profile and density of states for this RTD are shown in Figure 2. In order to correctly model the Γ-X coupling which occurs in this device we implement the sp3s* bandstructure model[2,3]. Simulated current density as a function of applied bias is shown in Figure 3 for both the analytic and numerical calculations. For this structure the analytic current density lies within 10% of the numerically determined current density. This is roughly within the precision of the predictive capabilities of these models. Therefore, this technique is very useful to obtaining qualitatively correct current densities with minimal computational overhead.

In Figure 4, we compare the sp3s* result to experimental data and a single band effective mass simulation. The single band result significantly underestimates the experimental current density. Since

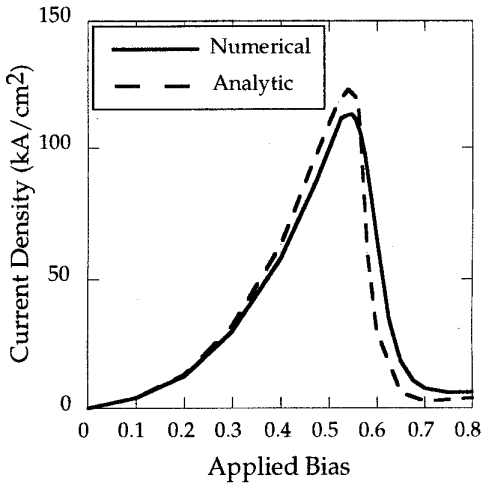

FIG. 3. Numerical (solid line) and analytic (dashed line) current density vs. applied bias for the GaAs/AlAs RTD.

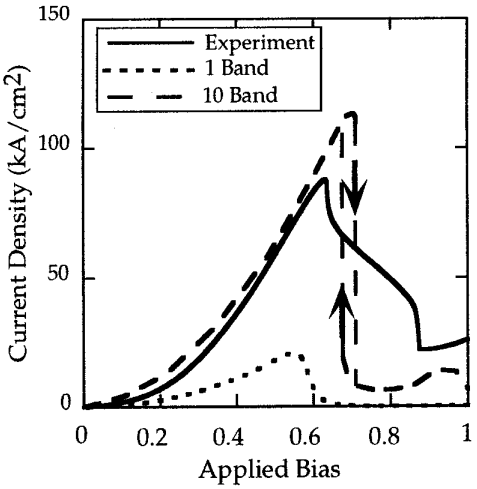

FIG. 4. Comparison between single band, multi-band, and experimental J-V curves for the GaAs/AlAs RTD. Additional current density predicted by the multiband model is due to the non-parabolicity of the imaginary band and conduction channels due to X-states in the AlAs barrier.

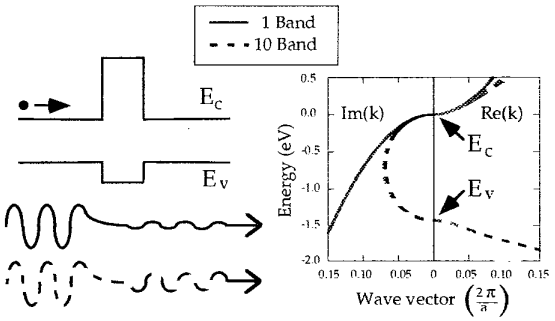

FIG. 5. Right: Complex band structure of AlAs for single band and multiband models. In the multiband model, the imaginary band connects with the light hole valence band (other valence bands have been omitted for clarity). Thus, the decay constant for electrons tunneling through this barrier is smaller than that predicted by the single band model. The result is that the single band model predicts the barrier to be more opaque than reality. Left: Illustration of the relative tunneling transmission of single and multi band models.

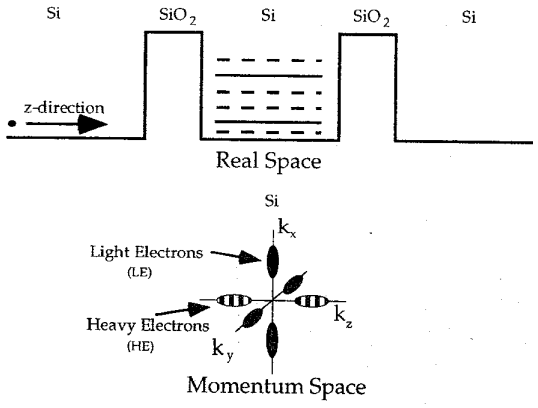

FIG. 6. Resonant states in a Si/SiO_2 RTD. Since the well material is indirect, there exists a superposition of two resonance spectra. One of these is derived from the longitudinal valley states (dashed lines) and the other is derived from the transverse valley states (solid lines).

the sp3s* result is much closer to the experimental value we may conclude that this is due to full bandstructure effects. Note that series resistance has been included in the simulated curves. This accounts for the bi-stability seen in the multiband curve.

One of the bandstructure effects that accounts for the difference between the two models is the strong non-parabolicity of the imaginary in the AlAs barrier. As shown in Figure 5 the single band model predicts that this band is parabolic and the decay constant increases with decreasing energy (referenced from the top of the barrier). However, this imaginary band actually connects with the light-hole valence band rendering it highly non-parabolic. Therefore, if the valence band is not included in the model, the AlAs barrier appears more opaque to tunneling than reality.

The other important bandstructure effect in this device is X-valley transport in the barrier. As is shown in Figure 2, the X-point conduction band profile for a GaAs/AlAs/GaAs heterostructure forms a quantum well possessing bound states. Since the longitudinal momentum is not conserved in heterojunctions, these bound X-states couple to the continuum states in the contacts. Therefore, additional resonant channels are available in the AlAs barrier via bound X-states. These channels are evident in the density of states plotted in Figure 2. Both of these phenomena account for the higher current density predicted by the full bandstructure model in Figure 4.

We have also calculated current densities in a Si/SiO_2 resonant tunneling diode. Since Si is an indirect gap material, we must use a bandstructure model which accurately represents the lowest conduction band throughout the entire Brioullin zone. We have chosen to use the four band, 2nd nearest neighbor anti-bonding orbital model developed by Chang[4]. The bandstructure of SiO_2 was obtained using an ab-initio pseudopotential method assuming the β-crystobalite structure. The anti-bonding orbital matrix elements were adjusted to match the ab-initio pseudopotential bandstructure.

As shown in Figure 6, the Si RTD possesses a superposition of two resonance spectra. One of these is due to states derived from the longitudinal valleys (Heavy Electrons $m^* = 0.91m_0$) and the other is due to states derived from the transverse valleys (Light Electrons $m^* = 0.19m_0$). The 2D (transverse) density of states for the light electrons (LE) is a factor of nine greater than that of the heavy electrons (HE). Assuming that the decay constants in SiO_2 are similar in both regions of the Brillouin zone, one expects that the current in this structure to be dominated by the LE resonance spectrum.

The analytically calculated current density vs. applied bias for the Si/SiO_2 RTD is shown in Figure

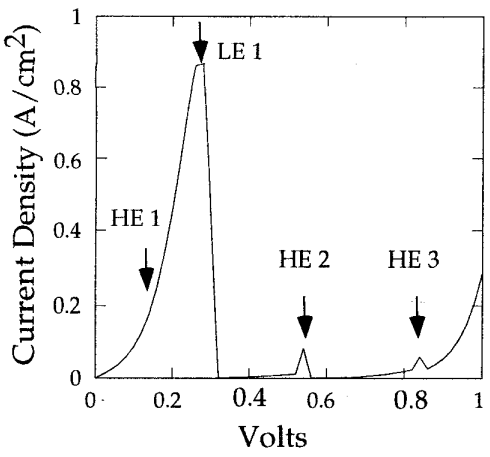

FIG. 7. Analytically calculated J-V curve for the Si/SiO_2 resonant tunneling diode. The main peak is due to the light electron (LE) resonance. Fine structure in the valley current is due to heavy electron (HE) resonances.

7. In this structure, the difference between the numerical and analytic current densities is on the order of 0.01%. This is due to the fact that the resonance linewidths in the Si/SiO_2 RTD are extremely narrow (nano eV). Therefore, nearly all of the current flows in a small energy range near resonance. Since the rational function approximation is accurate near resonances, the analytic J-V is accurate for devices with narrow resonance features such as the Si/SiO_2 RTD. The main peak of the J-V curve is due to the ground LE state in the quantum well. The HE resonances produce fine structure in the valley current of the J-V curve.

III. CONCLUSION

We have developed efficient numerical techniques to locate resonances and analytically calculate current densities in quantum devices using full band-structure models. These have been demonstrated by simulating both GaAs/AlAs and Si/SiO_2 resonant tunneling diodes. The analytic calculation of current density is most accurate for devices possessing narrow resonance widths such as the Si/SiO_2 RTD. The strength of this method lies in its ability to provide users with a qualitative and in many structures quantitative current-voltage characteristic in a few minitues of CPU time of present day workstations. This technique has been incorporated into an interactive multiband quantum device design tool.

Acknowledgements We acknowledge the benefit of discussions with Alan Seabaugh, Roger Lake and Shaoping Tang.

[1] R. C. Bowen, W. R. Frensley, G. Klimeck, and R. K. Lake, Phys. Rev. B **52**, 2754 (1995).
[2] P. Vogl, H. P. Hjalmarson, and J. D. Dow, J. Phys. Chem. Solids **44**, 365 (1983).
[3] T. B. Boykin and J. S. Harris, J. Appl. Phys **72**, 988 (1992).
[4] J. C. Chiang and Y. C. Chang, J. Appl. Phys. **73**, 2402 (1993).